Spiral Image Fusion by Interchannel Autowaves

Jason M. Kinser
Institute for Biosciences, Bioinformatics, and Biotechnology
George Mason University, 4E3
Manassas, VA 20110
jkinser@gmu.edu

Abstract

With the onset of inexpensive 2D optical detector arrays, digitized image information is readily available. Some systems, such as AOTF systems, produce up to 256 parallel channels of image information. These hyperspectral data cubes contain portions of target information in
separate channels. Rarely, does a single a channel contain sufficient target information. Inter-channel linking of pulse image generators is capable of segmenting the many channels in concert. Spiral image fusion occurs by phase-encoding pulse images and analyzing through
complex fractional power filters.

1. INTRODUCTION

An imaging sensor suite has the ability to generate several spectral images of a scene. These images are stacked together to form an image cube. The task of image analysis software is to extract from this data cube the detection of a target. This is not an easy task since quite often the target exists only partially in any single channel.

This paper will demonstrate a technique based upon the Pulse-Coupled Neural Network (PCNN) that allows for interchannel autowaves. These autowaves trigger events in neighboring channels which allows for the synchronization of pulses amongst channels. This synchronization segments the images from several channels, thus providing the foundation for target recognition.

2. THEORY

The theory of spiral image fusion begins with the PCNN [Kinser,97] [Kinser,98]. This system uses one PCNN per input channel. These PCNNs creating autowaves that synchronize behavior within each channel. These are intrachannel autowaves and have been the foundation for image segmentation. [Kinser,96] This system will allow these autowaves to cross channels and synchronize activity amongst the channels. A schematic of this system is shown in Fig. 1.

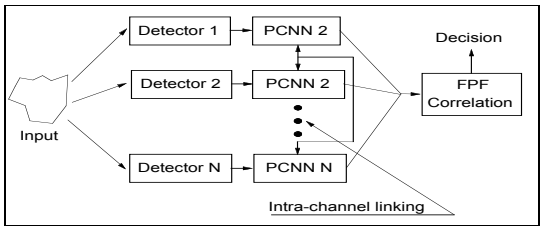

Fig. 1. Schematic of Spiral Image Fusion System.

Each PCNN creates a pulse image which have only binary elements. These images are then combined by phase encoding to create a single complex image that is filtered by the Fractional Power Filter (FPF) [Brasher,94]. The result of the filtering is strong correlation signals at the locations of the target. These steps are explained in the following sections.

2.1. PCNN Basics

The PCNN is a model based strongly on the Eckorn theory of the visual cortex. [Eckhorn,90] In this system neural interactions are second order and only local. The PCNN receives a stimulus, **S**, and through iterations produces several output pulse images. The computations cycle the following equations:

$$F_{ij}[n] = e^{-\alpha_F \Delta_h} F_{ij}[n-1] + S_{ij} + V_f \sum_{kl} M_{ijkl} Y_{kl}[n-1] \quad , \tag{1}$$

$$L_{ij}[n] = e^{-\alpha_L \Delta_h} L_{ij}[n-1] + V_L \sum_{kl} W_{ijkl} Y_{kl}[n-1] \quad , \tag{2}$$

$$U_{ij}[n] = F_{ij}[n]\left\{1 + \beta L_{ij}[n]\right\} \quad , \tag{3}$$

$$Y_{ij}[n] = \begin{cases} 1 & if\ U_{ij}[n] > \theta_{ij}[n] \\ 0 & Otherwise \end{cases} \quad , \tag{4}$$

$$\theta_{ij}[n] = e^{-\alpha_\theta \Delta_h} \theta_{ij}[n-1] + V_\theta Y_{ij}[n] \quad , \tag{5}$$

where F are the Feeding, L are the Linking compartments. U represents the internal states, Y are the outputs and θ are the dynamic thresholds. **M** and **W** are the local interneuron communications. The rest of the terms are scalars.

A typical example of the PCNN's ability to segment images in shown in Figs. 2. The segmentation is evident. For example, the ball, the face, the arms, the eyes, the arm of the chair, etc. are all segmented as pulse segments in differing output iterations. This segmentation is quite usual for target recognition. For example, if the target of interest was a face, then it would be far easier to detect the target in Fig. 2c than in 2a. This is due to the

fact that the target in 2c has extremely sharp edges which will spread the information about the target shape throughout the Fourier plane (which is the space where most filtering, including the FPF, occurs).

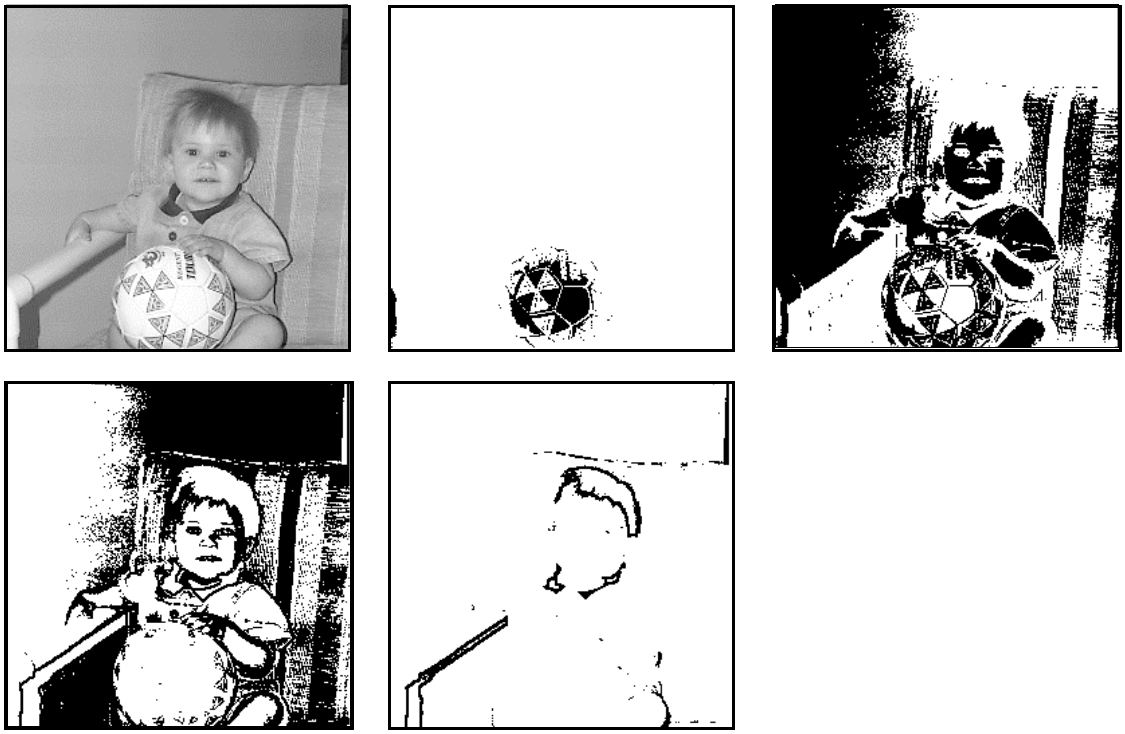

Figs. 2. An original input and the resulting PCNN outputs.

1.2. PCNN

The mathematical alterations to the original PCNN required to accomplish the inter-channel autowaves is shown in the following equations.

$$F_{ij}[n] = e^{-\alpha_F \Delta t} F_{ij}[n-1] + S_{ij} + V_f \sum_{kl} M_{ijkl}\, Y_{kl}[n-1] \quad , \tag{6}$$

$$L_{ij}[n] = e^{-\alpha_L \Delta t} L_{ij}[n-1] + V_L \sum_{kl} W_{ijkl} Y_{kl}[n-1] \quad , \tag{7}$$

$$U_{ij}[n] = F_{ij}[n]\left\{1 + \beta L_{ij}[n]\right\} , \tag{8}$$

$$Y_{ij}^{\theta}[n] = \begin{cases} 1 & if\ U_{ij}^{\theta}[n] > \Theta_{ij}^{\theta}[n] \\ 0 & Otherwise \end{cases}, \tag{9}$$

$$\Theta_{ij}^{\theta}[n] = e^{-\alpha_\theta} \Theta_{ij}^{\theta}[n-1] + V_\theta Y_{ij}^{\theta}[n] , \tag{10}$$

Each channel now has its own F, L, U, Θ, and Y. Furthermore, autowaves are now allowed to cross channels through $\mathbf{M}^{\theta}$ and $\mathbf{W}^{\theta}$.

A typical three channel example is shown in Figs. 3. The outputs are gray encoded with three levels of gray each representing a different channel. Outputs are not mutually exclusive.

Figs. 3. Gray scale version of a 3 channel (RGB) image and the gray encoded outputs of a 3 channel PCNN.

The effect of the interchannel autowaves are quite evident by examining a large segment of the image such as the boy's hair. It is brown and lighter at the top due to illumination gradients. Brown is expressed more in the red channel and therefore the red channel autowave is created first. It progresses from the lighter region of the hair downwards. However, this autowave has also triggered activity in the other channels and the green and blue autowaves follow the red wave respectively.

The outputs of the parallel PCNNs are shown here as combined gray scale images. In the spiral fusion system they are combined by phase encoding by

$$\mathbf{Y}^{T} = \sum_{\theta} \mathbf{Y}^{\theta} e^{j2\pi\theta/N} , \tag{11}$$

where $\mathbf{Y}^T$ is now the combined output of all channels. Since each channel can produce only binary elements, the elements of $\mathbf{Y}^T$ are still limited in values. It should be noted that there is not a loss of information in Eq. 11. Given $\mathbf{Y}^T$ it is possible to reconstruct all $\mathbf{Y}^{\theta}$'s.

The phase encoding is used instead of the gray encoding due to the behavior of the FPF. If the outputs were stacked to form an output data cube, then the global phase factors, θ, would create a helix or 'spiral' which is the foundation for the name of the system.

1.3. Fractional Power Filter

The Fractional Power Filter (FPF) is a composite filter that has the ability to manipulate the inherent trade-off between generalization and discrimination. It can train on many images with differing associated outputs. The training of a filter, **H**, from a set of Fourier images, **X**, is

$$\vec{H} = \mathbf{D}^{-1}\mathbf{X}\left[\mathbf{X}^T\mathbf{D}^{-1}\mathbf{X}\right]^{-1}\vec{c} \quad , \tag{12}$$

where

$$D_{ijkl} = \frac{\alpha_{ijkl}}{N}\sum_n |X_{n,ij}|^p \quad , \tag{13}$$

and **c** is the constraint vector set by the user. Basically, a training image **x** compared to the image space filter **h** will produce the corresponding element in **c**,

$$\left\langle \mathbf{h} \middle| \mathbf{x}^k \right\rangle = c_k \quad , \tag{14}$$

where k indicates the k-th image $\mathbf{x}^k$ and the k-th element of the constraint vector, c_k.

To complete the spiral image fusion system, an FPF is created to identify the target. In the case Figs. 3 a filter could be created to find the ice cream. Now all of the parts of the system are created.

1.4. System Operation

Operation of the system follows the diagram in Fig. 1. A multi-channel input stimulus is presented to parallel PCNN's and each of these cooperatively produce output pulse images which are combined as in Eq. 11. The combined outputs are then compared to a filter. Large correlation signals from this comparison indicate the presence and location of the target.

2. EXAMPLES

The spiral image fusion system has been applied to a few examples.

2.1. Landmine Detection

In this example the input had 30 spectral channels all in the IR. [Kinser,98] The input consisted of two landmines sitting on a table near a Halogen calibrator. The landmines had features (spokes or rings) that were difficult to detect. Figs. 4 display two of the original input channels (longest wavelength, and shortest wavelength) and two of the gray encoded pulse image outputs. Note that the two landmines (center of the images) have distinctive features in the pulse images that are difficult to distinguish in the original inputs.

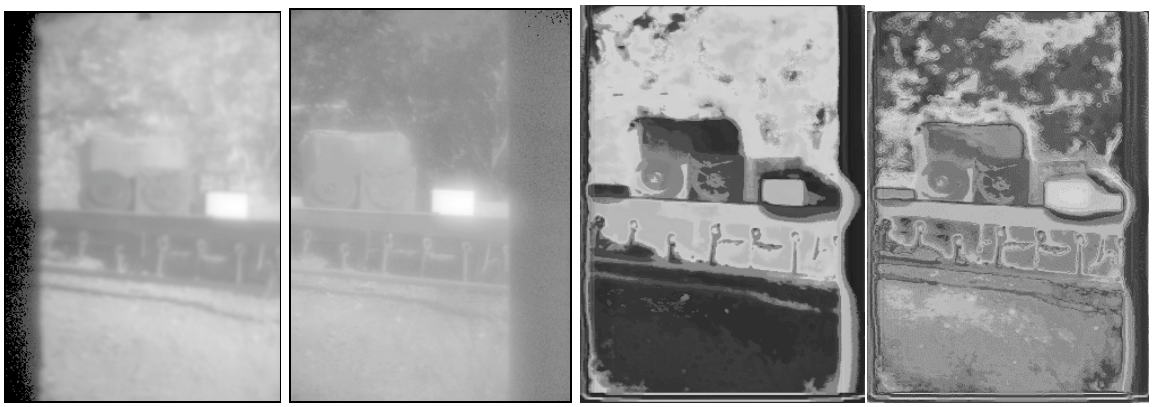

Figs. 4. Two of the input channels and two of the gray encoded output pulse images.

To demonstrate this system an FPF was created that would attempt to detect only the landmine with spokes. Fig. 5 displays a plot of the results. These plots are for two different cases. The first case is an attempt to detect the landmine from a single channel (#20 was chosen since it had to most distinctive presentation of the landmine). The correlation of the filter produced a 2D correlation surface. The plot shown is a single slice through the target location of that correlation surface. If the filter had detected the landmine there would have been a peak in the middle. As can be seen, this filter failed.

The second plot is that of the spiral image system. Here a peak is seen and the target was detected. Similar results were obtained when the other landmine was chosen to be the target.

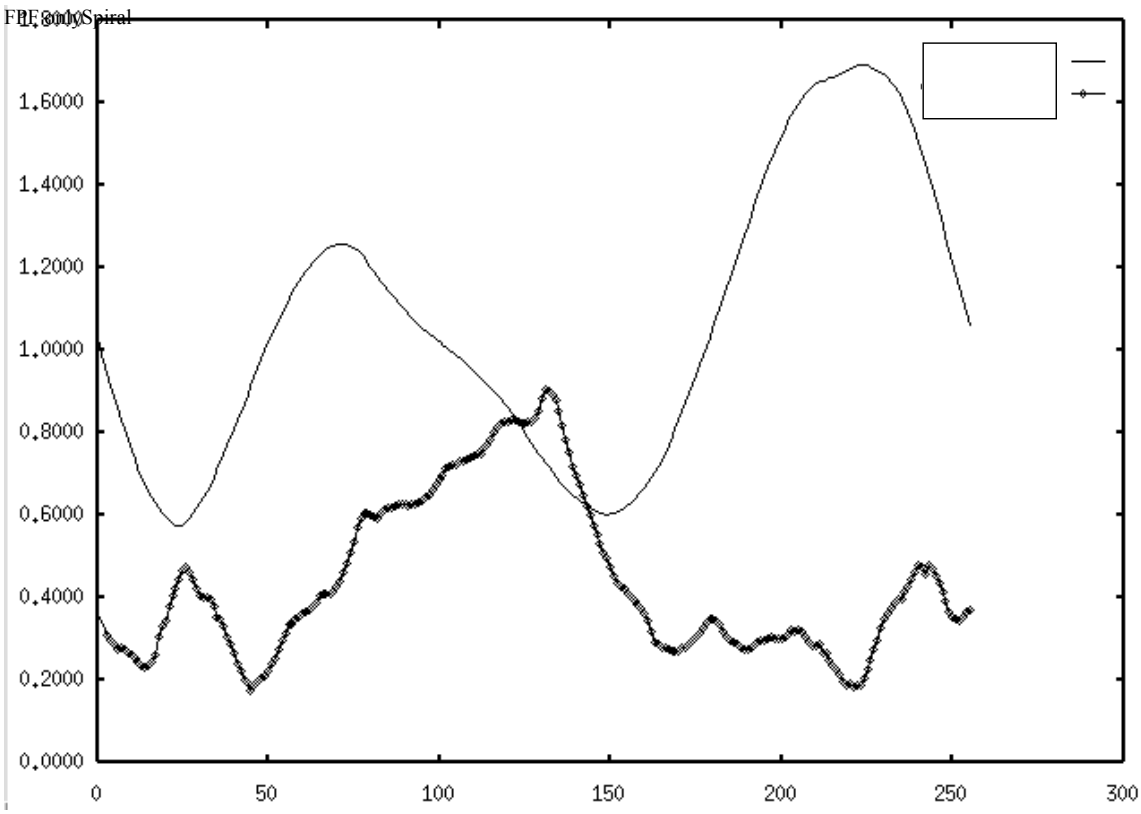

Fig. 5. Plots of correlation surface slices from two tests: traditional filtering and spiral image fusion filtering.

2.2. Mice: Niemann Pick-C Disease.

Another case involved a detector at the National Institutes of Health producing 256 parallel channels of IR images. The challenge was to find differences in the brains of mice with and Niemann Pick-C disease to those without. The manifestation of this disease in the images is not well understood.

Figs. 6 display the same iteration from four different samples. These again are the gray encoded combination of the pulse outputs of all channels. Figs. 6c and 6d are normal mice. There do exist texture and edge differences between the normal and diseased. However, from this small data set no conclusions are drawn. These images are displayed merely to demonstrate the output of a 256 channel PCNN.

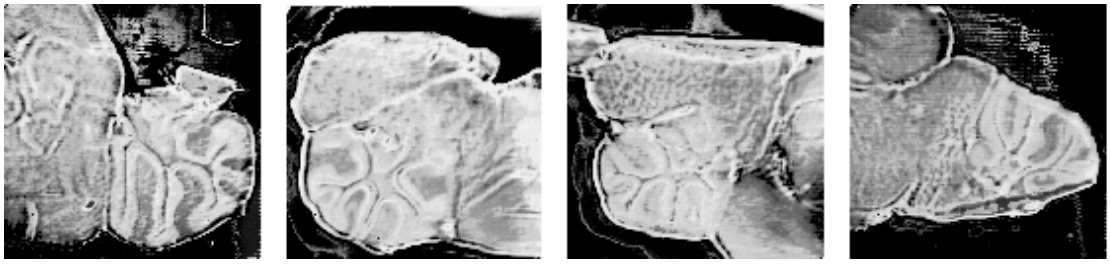

Figs. 6. Outputs from an PCNN for four different cases.

3. SUMMARY AND FUTURE RESEARCH

The spiral image fusion theory was presented. This system uses inter-channel autowave communication to synchronize pulse activity in the different channels. Then the system iteratively produces a set of phase-encoded images that can be filtered to detect targets.

This research is not complete. Certainly, the simple examples demonstrated here do not demonstrate the limits and/or abilities of this system. Future directions of research would include a more exhaustive study.

The signal fusion community also spends a great deal of time attempting to thwart co-alignment problems. In the examples shown here all of the channels were aligned. Data is not usually produced in such a nice set. Given known alignment parameters it would be possible to warp **M** and **W** to accommodate the misalignments. Future research would consider non-symmetric inter-neural connections to accommodate misaligned input channels.

4. REFERENCES

J. Brasher and J. M. Kinser, "Fractional-Power Synthetic Discriminant Functions", Pattern Recognition **27**(4), 577-585 (1994).

R. Eckhorn, H. J. Reitboeck, M. Arndt, P. Dicke, "Feature Linking via Synchronization among Distributed Assemblies: Simulations of Results from Cat Visual Cortex", Neural Computation **2**, 293-307, (1990).

J. M. Kinser, "Object Isolation", Optical Memories and Neural Networks, **5**(3), 137-145 (1996).

J. M. Kinser, "Pulse-Coupled Image Fusion", Optical Eng., **36**(3), 737-742 (1997).

J. M. Kinser, C. L. Wyman, B. Kerstiens, "Spiral Image Fusion: A 30 Parallel Channel Case", Optical Eng. **37**(2), 492-498 (1998).